BALLISTIC DAMAGE VISUALIZATION & QUANTIFICATION IN MONOLITHIC TI-6AL-4V WITH X-RAY COMPUTED TOMOGRAPHY

J.M. Wells[1], W.H. Green[2], N.L. Rupert[3], J.M. Winter, Jr.[4] , J.R. Wheeler[5] , S.J. Cimpoeru [6], and A.V. Zibarov[7]

[1] JMW Associates, 102 Pine Hill Blvd, Mashpee, MA 02649-2869
[2, 3] US Army Research Laboratory, Weapons & Materials Research Division, AMSRL-WM-MB[2]/-TD[3], APG, MD 21005-5069
[4,5] ORISE Contractor at WMRD, ARL, MD 21005-5069
[6] DSTO Melbourne, 506 Lorimer St, Fishermans Bend, 3207, Australia
[7] GDT Software Group, Revolutsil St, 28-49, 300034, Tula, Russia

ABSTRACT This paper addresses the investigation of the in situ volumetric internal ballistic damage of monolithic Ti-6Al-4V alloy V_{50} targets using X-ray Computed Tomography, XCT. The interrogation was conducted with individual XCT scans of ~ 0.5 mm thickness to reveal 3D volumetric damage larger than the minimum feature resolution limits (> 0.25 mm). Image processing and visualization techniques utilized include contiguous 2D scan sequencing, reconstructed 3D solid objects and virtual sectioning, and recently developed colorized point cloud imaging which more clearly allows visualization of the volumetric damage network by making the matrix itself transparent. Additionally, new methods to quantify the volumetric axi-symmetric damage fraction are introduced. Observed damage features include multiple meso-scale cracks and voids. Of particular interest is the distinct and interesting meso-scale cracking morphology described herein as "spiral orbital cracking" located beyond the penetration cavity in the exit half of the sample.

INTRODUCTION

In order to facilitate the development of light weight armor systems utilizing titanium alloys, one needs to establish improved methodologies for *in situ* characterization and visualization of the internal damage which occurs during ballistic impact. Too frequently, post-impact diagnostics have been mainly concerned with the extent of penetration and much less conserned with detail of the damage that surrounds the penetration cavity, both in instances of complete, as well as partial, penetration. Ideally, it is desirable to predict *a priori* the nature, extent, and morphology of the impact damage in the titanium target material following impact from threats of variable severity. It is also considered useful to have the demonstrated capability of actually characterizing the details of such impact damage to either verify or assist in the development of future predictive impact damage models.

The nondestructive technique of industrial X-ray Computed Tomography, XCT, is utilized by the authors [1-3] to significantly improve our diagnostic capabilities by

providing the desired information to detect, locate, characterize, and visualize the impact damage in 3 dimensions (3D) in samples from impact targets of titanium alloy Ti-6Al-4V. While destructive sectioning and polishing has the distinct advantage of being able to observe target material micro-structural and damage features at higher resolution levels than presently attainable with XCT, there are, however, several functional advantages of XCT over destructive sectioning including:

a) XCT is a ***reversible*** process using virtual sectioning where the sectioned target material can be restored and then re-sectioned on different planes without penalty. No unintentional incipient damage is introduced into the sample during processing. Also, the subject object retains its original form and function if desired for further testing or subsequent service utilization as could be the case for various military components.

b) Image processing software permits the virtual reconstruction of the digital XCT image into a variety of 2D multi-planar reconstructions and 3D solid objects, with arbitrary virtual sectioning as desired. Selected features such as voids or cracking networks can be virtually isolated and visualized in 3D as transparent point clouds entirely independent of the opacity of the original target material.

c) XCT provides the only high resolution, non-destructive approach available to completely interrogate, capture and discriminate internal damage features throughout the entire 3D voxel volume of the target object. Results are obtained as direct XCT scans, reconstructed qualitative images and quantitative measurements of selected features. Resulting data can be stored and/or exported in several engineering formats.

X-RAY COMPUTED TOMOGRAPHY EXAMINATION

The initial ballistics study on the present Ti-6Al-4V samples was described previously by Cimpoeru *et al.* [4]. Relatively little utilization of the XCT technology has occurred to date in the study of ballistic damage assessment of armor materials. DeLuca *et al.* [5] published an earlier study of impact damage using XCT in organic S2-glass reinforced plastic structural armor material. Wells, Green and Rupert [1,2] have reported on the use of XCT in the assessment of both pre- and post-ballistic impact damage in various inorganic armor ceramics including TiC, TiB_2, Al_2O_3 and SiC and on the early XCT examination of these same Ti-6Al-4V samples [3].

The present work further develops this technique for improved 3D visualization and characterization of internal ballistic damage morphology in a monolithic metallic target system. Selected perforated samples of Ti-6Al-4V alloy were examined utilizing the 420 keV XCT facility at the ARL in Aberdeen Proving Ground, MD. First by digital radiographs, DR, revealing the through thickness profile of the penetration cavity and then by XCT scanning perpendicular to the projectile flight direction from the impact face to the exit face sequentially in contiguous incremental slices of ~ 0.5mm thickness.

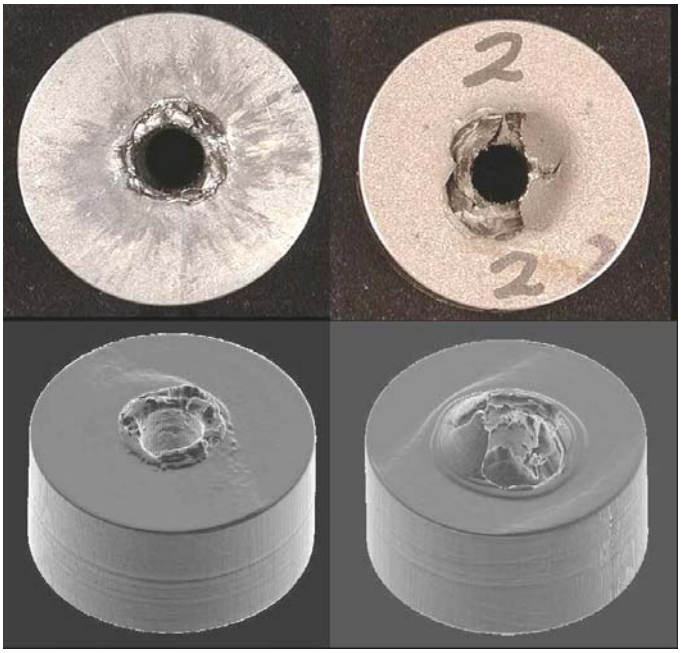

Figure **1.** Macrophotographs of the 50 mm diameter APM2 sample #2 are shown (top) and the respective 3D XCT virtual solid object reconstructions (bottom) of both the impact (left) and exit (right) faces.

Macro-photographs of the impact and exit faces are shown above their respective reconstructed 3D solid images of APM2 sample #2 (impact velocity 702 ms^{-1}) in Figure 1. Note that considerable depth of detail into the penetration cavity is observed in the images of the 3D XCT virtual solid object reconstructions of both the impact and the exit surface, respectively. Also, additional topological detail can be observed about the penetration cavity in each of the 3D solid object images than in the 2D macro-photograph images directly above.

In addition to the central penetration cavity, two basic meso-scale damage defect forms are observed in the 2D XCT scan of axial slice #45 shown in Figure 2, namely scattered damage voids and prominent larger orbital cracking segments. The two later ostensibly unconnected damage features observed in Figure 2 are mainly located in the lower half of the samples toward the exit face. When one observes this damage in the digitized XCT scans in consecutive sequence, a further feature of the orbital cracking becomes readily apparent, namely a pronounced clockwise spiral rotation towards the exit face. This spiral rotation may be seen in the five contiguous XCT slice images shown in Figure 3 where a dashed radial line is drawn through the approximate center of each orbital arc segment. The clockwise rotation of this line is clearly observed as one advances along successive XCT slices (#36 to #40) spaced ~ 0.5 mm apart toward the sample exit face. Similar results were obtained in all six of the APM2 samples that were analyzed.

Figure 2. Individual XCT axial scan #52 of Ti-6Al-4V APM2 sample#2 showing several small damage voids and two larger curved orbital cracking segments seemingly without being connected to the ballistic cavity. Axial slice is ~ 4 mm from the exit face.

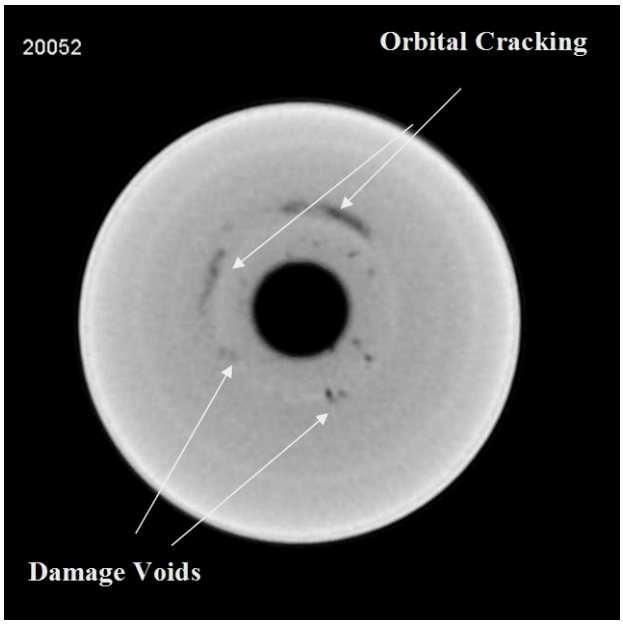

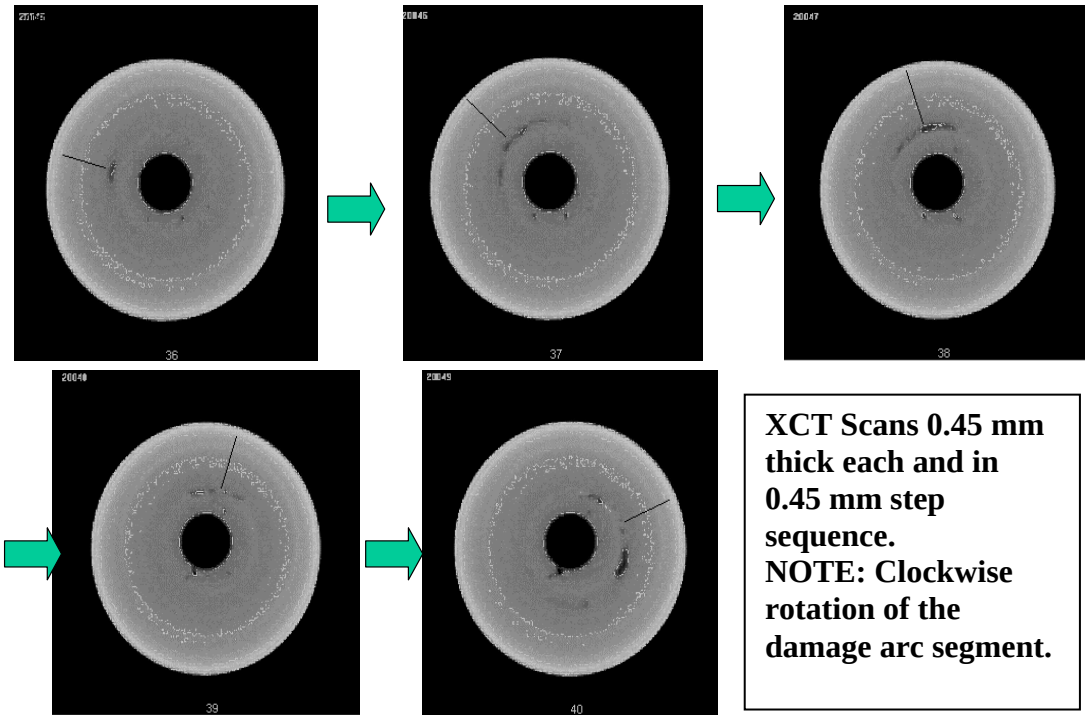

FIGURE 3. Five contiguous XCT slices within APM2 sample#2 showing the clockwise spiral rotation of orbital cracking arcs.

RECONSTRUCTED IMAGING AND DAMAGE VISUALIZATION

Further details of the observed damage beyond the radius of the ballistic cavity are revealed by virtual sectioning of the reconstructed 3D solid images of an individual sample. In this instance, arbitrary slices are made parallel to the ballistic cavity through the entire sample thickness. A series of such virtual slices was reconstructed from the XCT database at several selected radii from the center of the ballistic cavity. Figure 4 reveals two such virtual slices, one through the approximate center and the second near the radius of the ballistic cavity in APM2 sample #2. Most of the observed damage of interest appears in the lower half of these figures near the exit face. The cracking features observed on both sides of the penetration cavity are shown in the circled areas and appear of several millimeters in

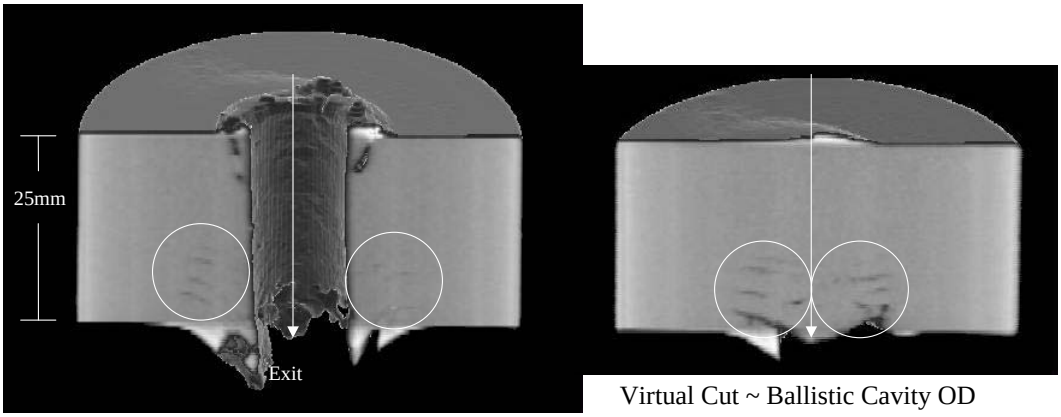

FIGURE 4. Virtual slices through a 3D solid object reconstruction of APM2 sample #2 showing ballistic damage beyond the cavity radius. Arrow indicates projectile direction from impact toward exit face.

length and with an orientation either as horizontal or slightly tilted downward toward the cavity center on the exit face. This cracking is an apparent manifestation of a discing failure mechanism mentioned that forms due to fractures along various planes of weakness in the through-thickness direction [6].

Further connectivity at a crack size less than the ~ 250 μm resolution achieved with XCT was observed in metallographic sections of the same sample, that were polished and etched (using a Nitric Acid/HF enchant). Full grinding and polishing of the specimen in the direction of penetration was accomplished at DSTO in sequential 1mm steps starting at the exit face. Each resulting full cross sectional surface was polished to 1200 grade paper and lightly etched and photographed. Figures 5(a) and 5(b) show two magnifications of a cross sectional images at ~9 mm from the exit face. The through-thickness section shown in Figure 5(c) reveals how the fracture surfaces orient and how the plastically deformed zone

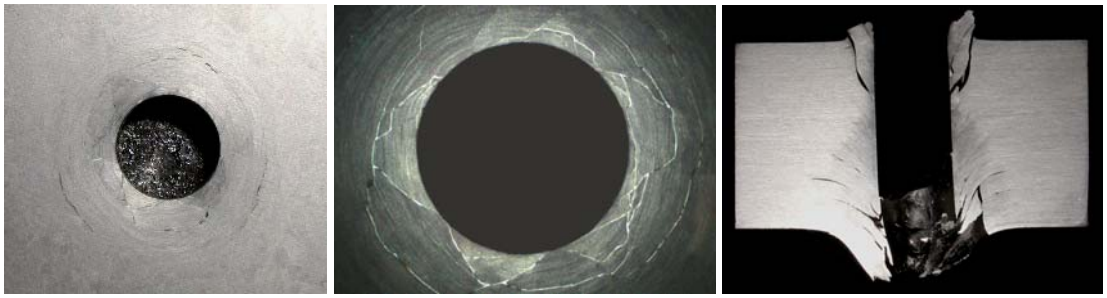

(a) (b) (c)

FIGURE 5. Macro-photographs of cross sections: of APM2 sample #2 (702 ms^{-1}) at a distance 9 mm from the exit face (a) polished section, (b) polished and etched section showing the shear bands and small cracks connecting the meso-scale orbital cracks with the penetration cavity, and (c) view of polished and etched cross section of APM2 sample #9 (682 ms^{-1}) [3].

that contains the shear bands appears to increase significantly in size as the exit face is approached. A plastic zone that increases in diameter with increasing penetration depth (~14 mm maximum radius) surrounds the penetration cavity. Interestingly, orbital cracking segments are observed at or near the outer boundary of the plastic zone. Shear bands in the plastic zone surrounding the penetration cavity Figure 5(b) reveal that the crack segments are simply visible portions of shear failure connected by adiabatic shear bands.

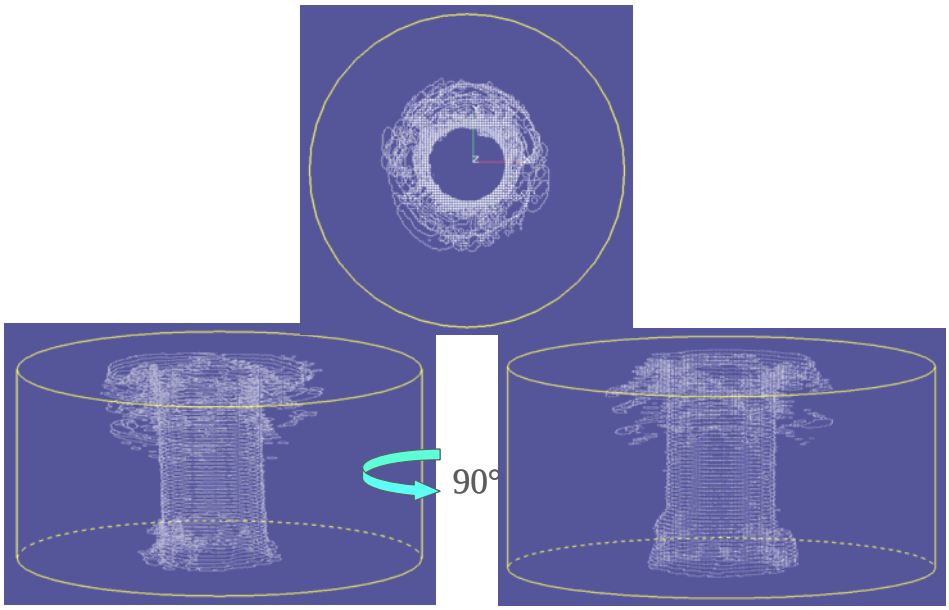

Figure 6. Transparent point cloud images showing internal damage within Ti-6Al-4V APM2 sample #2 from top, front and side views. Exit face is at top of these images.

Further processing of the entire sample XCT scan data file involved threshold segmentation and isolation of the damage data and reconstruction of virtual transparent point cloud images at ARL as shown in Figure 6. In this figure, one observes: (a) the radial extent of damage and (b) the localization of the orbital cracking outside of the penetration cavity as the exit face is approached. Additionally, one can observe clear indications of the spiral nature of the orbital cracking. Additional virtual transparent point cloud images were reconstructed using GDT ScientificVR(c) visualizer software with more sophisticated variable 3D transparency and artificial colorization techniques to more clearly reveal the *in situ* orbital cracking morphology in this same APM2 sample #2. These additional point cloud images are shown in Figure 7. The visualization of the impact damage shown in Figure 6 is considered further improved by reconstructing the theshold damage data using the GDT software with results shown in Figure 7.

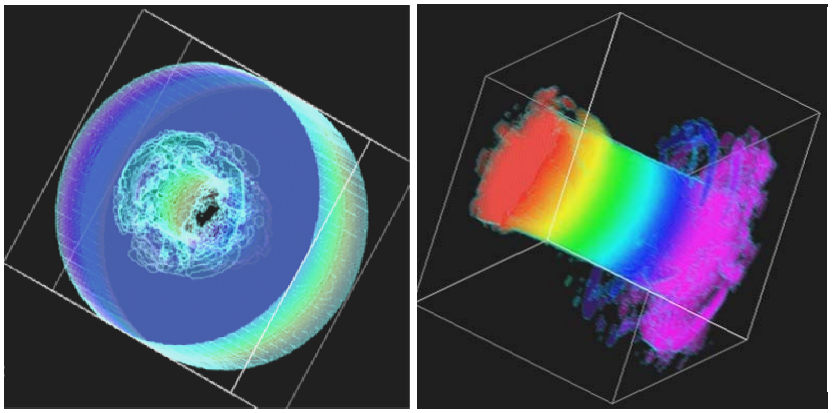

Figure 7. Transparent Point cloud images from GDT Software Group showing internal impact damage within APM2 sample #2. LHS image shown with semi-trans-parent matrix and RHS with fully transparent matrix Ti-64 material.

QUANTITATIVE DAMAGE VISUALIZATION

Initial results of the quantification of the volumetric impact damage in samples APM2 #2 & #4 are shown in Figure 8. The axi-symetrical damage fraction is plotted versus radius (in mm) from the center of the penetration cavity and along the entire penetration depth from the entrance to the exit face. The Z-axis labeled “Depth“ is scaled according to the numerical sequencing of the XCT axial slices, staring with #10 at the impact face and #60 at the exit face of each APM2 sample. The depth of each slice is 0.5 mm thick. The Unit Damage Fraction parameter being plotted as the ordinate can be defined as the normalized damage fraction measured as the ratio of damage pixels (actually voxels) in a torordal ring from the edge of the penetration cavity incrementally out to the sample radius with the oriin at the center of the cavity. These measurement are repeated for each axial slice through the entire axial scan data set. No account is made of the angular orientation of the damage segment within a torordal ring segment at each radius in the measurements shown in Figure 8. Further details of this quantification approach can be found elsewhere in this conference in the paper by Wheeler et al.

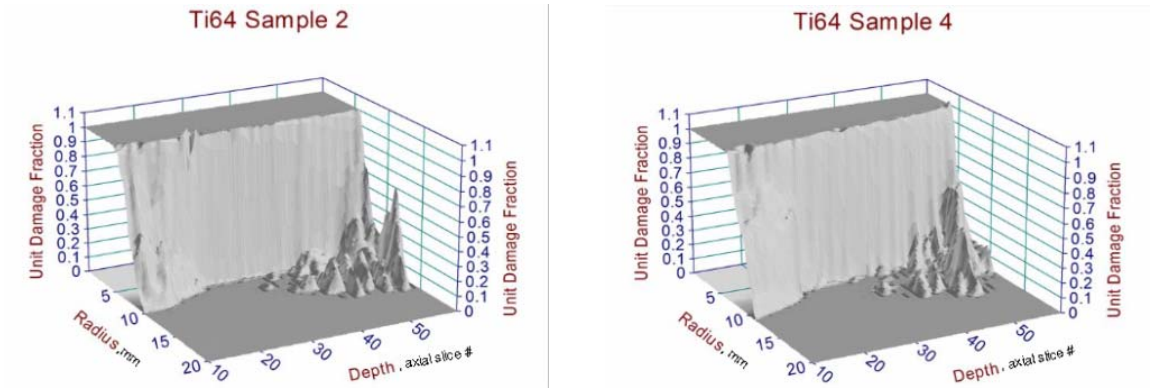

Figure 8. Quantitative visualization of axi-symetrical damage function in APM2 samples #2 & #4 plotted against radius and penetration depth data taken from original XCT scans.

CONCLUSIONS

The authors have provided several different 3D virtual images, as well as original 2D XCT scans, of ballistic impact damage in a monolithic Ti-6Al-4V alloy target. Beyond the through thickness penetration cavity, the most prominent and remarkable damage feature is that of a prominent orbital spiral cracking morphology concentrated to within ~ one projectile diameter of the target thickness near the exit face. This damage is constrained radially to within ~ 2.5X the radius of the penetration cavity. While this damage appears to be physically unconnected to the penetration cavity in XCT images, further detailed metallographic examination convincingly demonstrates fine scale physical connectivity but that is below the resolution level currently available with XCT for samples of this size. Overall the XCT scans and analysis have enabled a comprehensive visualization and understanding of the failure mode and the extent of damage in perforated monolithic Ti-6Al-4V targets. This will aid in the development of improved predictive modelling techiques and improve our understanding of multi-hit capability of this material.

REFERENCES

1. J. M.Wells, W.H.Green, and N.L.Rupert, "Nondestructive 3-D Visualization of Ballistic Impact Damage in a TiC Ceramic Target Material", *Proceedings MSMS2001, 2nd International Conference on Mechanics of Structures*, University of Wollongong, Wollongong, NSW, Australia, 159-165, 2001.
2. J.M.Wells, N.L.Rupert, and W.H.Green, "Progress in the 3-D Visualization of Interior Ballistic Damage in Armor Ceramics", *Proceedings of ACERS PacRim IV Conference*, Maui, Hawaii, 441-448, 2001.
3. J.M. Wells, W.H.Green, N.L.Rupert, A.Cole, S.J.Alkemade, S.J.Cimpoeru and M.Szymczak, "Ballistic Damage Visualization In Monolithic Ti-6AL-4V with X-ray Computed Tomography", *20th International Symposium on Ballistics*, Orlando, Fl, ADPA, vol. 2, 1112-1120, 2002.
4. S.J. Cimpoeru, S.J.Alkemade, M.Szymczak, N.L.Rupert, W.H.Green and J.M.Wells, "Ballistic Assessment of a Low-Cost Ti-6Al-4V Titanium Alloy", *Australian J. of Mech. Engng*, 1(1), 5-9, 2003.
5. E.DeLuca, J.Prifty, W.Betheney, and S.C. Chou. "Ballistic Impact Damage of S2-Glass Reinforced Plastic Structural Armor", *Composites Science and Technology*, 58, 1453-1461, 1998.
6. R.L. Woodward, "The Interrelation of Failure Modes Observed in the Penetration of Metallic Targets", *Int. J. Impact Engng*, 2, 121-129, 1984.